

Synthesis and Spectral Properties of 1,8-Bridged Fluorenophanes Consisting of Polynuclear Aromatic Component

Akihiko Tsuge,* Ryosuke Nada, Tetsuji Moriguchi, and Kazunori Sakata

Department of Applied Chemistry, Kyushu Institute of Technology, Tobata-ku, Kitakyushu 804-8550, Japan

tsuge@che.kyutech.ac.jp

Received June 20, 2001

One of the most characteristic features of cyclophane compounds could provide information about intramolecular interactions by employing their defined arrangement of some components in the molecule.¹ During the course of our study on cyclophanes,^{2,3} the fluorene unit has been selected as the component of cyclic compounds because of its aromatic nature and acidic protons. We have developed a convenient method⁴ to synthesize the 1,8-bridged fluorenophanes and also examined their conformation, indicating that the orientation between the fluorene component and another aromatic component is characteristic of their molecular structure.

This result prompted us to investigate the intramolecular transannular interaction between the fluorene unit and the polynuclear aromatic component.

Thus, we now describe the synthesis of 1,8-bridged fluorenophanes consisting of naphthalene, anthracene or pyrene component, their conformation and their behavior of absorption and fluorescence spectra.

Results and Discussion

Cyclization of mercaptomethyl compound (**1a**⁴) and halomethyl compounds (**2a**,⁵ **3a**,⁶ and **4a**⁷) using CsOH as a base under highly dilute conditions afforded the corresponding dithiafluorenophanes (**5a**^{3–7a}) in 57–75% yields. After the oxidation of **5a–7a** with *m*-CPBA, the corresponding disulfones were subjected to pyrolysis at 500 °C under reduced pressure to give the desired fluorenophanes (**5b–7b**) in 25–40% yields (Chart 1).

The ¹H NMR spectra of the fluorenophanes could provide their conformational features; thus, the signals of the 9-protons and the bridge methylene protons are summarized in Table 1.

A singlet is observed for the 9-protons in **5a** and **6a** as a result of the fast flipping of the aromatic component at room temperature on the NMR time scale, which is consistent with two singlets for the bridge methylene

Chart 1

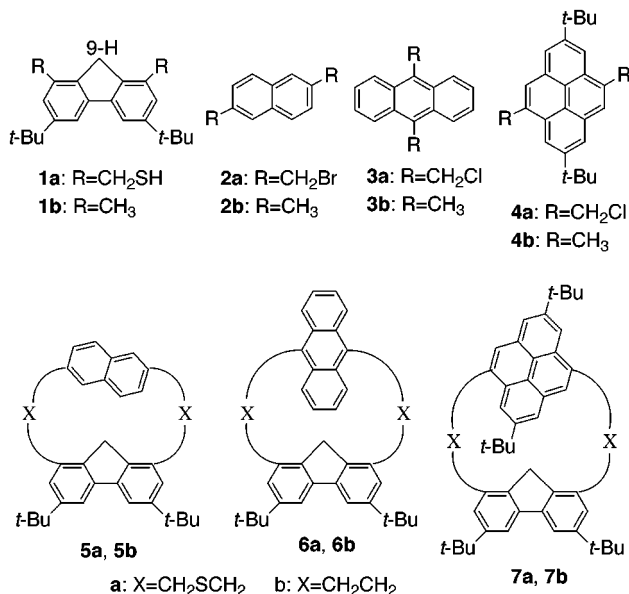


Table 1. Partial Chemical Shifts^a in Fluorenophanes

| compd | 9-proton (δ /ppm) | bridge proton ^b (δ /ppm) |
|-----------|---|--|
| 5a | 1.58 (s) | 3.22 (s), 3.65 (s) |
| 6a | 1.55 (s) | 3.69 (s), 4.95 (s) |
| 7a | -0.48 (d, $J = 21$) 1.40 (d, $J = 21$) | 2.94 (d, $J = 14$), 2.99 (d, $J = 14$) 4.24 (d, $J = 13$), 4.71 (d, $J = 13$) |
| 5b | -0.69 (d, $J = 21$) 2.11 (d, $J = 21$) | 1.61–3.28 (m) |
| 6b | -1.59 (d, $J = 21$) 1.83 (d, $J = 21$) | 2.27–4.31 (m) |
| 7 | -0.80 (d, $J = 21$) 1.59 (d, $J = 21$) | 2.80–4.09 (m) |
| 1b | 3.95 (s) | |

^a In CDCl₃ at 27 °C. ^b J/Hz.

protons. On the basis of the variable-temperature NMR technique, **6a** was found out to coalesce at -30 °C, corresponding to $\Delta G^\ddagger = 43$ kJ mol⁻¹ in contrast to the coalescence temperature at -50 °C for **5a**.³

On the contrary, the 9-protons and the bridge methylene protons in **7a** exhibit a doublet and two sets of doublets, respectively. No obvious changes in these signals were observed even at 150 °C, indicating that the conformation of **7a** is fixed. The pyrene component seems too large for inversion of the ring. A similar rigid structure has been confirmed for **5b–7b** on the basis of their NMR spectral behavior.

As shown in Table 1, one of two 9-protons in **7a** and **5b–7b** is subject to a large upfield shift in comparison with that of **1b**, which undoubtedly stems from the shielding effect of the opposite aromatic component. In any event, the 9-proton penetrates farther into the π -cavity of the aromatic component in these compounds. This plausible geometry is strongly supported by the X-ray analysis of **5b**⁸ in which the naphthalene ring is located right upon one of the 9-protons (Figure 1).

Some intramolecular interactions could be expected for the two chromophoric components present in the specific

(8) The X-ray crystallographic data for **5b** have been deposited with the Cambridge Crystallographic Data Centre as CCDC no. 162499.

(1) For example, see: (a) Vögtle, F. *Supramolecular Chemistry*; Wiley: Chichester, 1989. (b) Diederich, F. *Cyclophanes*; The Royal Society of Chemistry: Cambridge, 1991. (c) Vögtle, F. *Cyclophane Chemistry*; Wiley: Chichester, 1989.

(2) Tsuge, A.; Ueda, Y.; Araki, T.; Moriguchi, T.; Sakata, K.; Koya, K.; Mataka, S.; Tashiro, M. *J. Chem. Res., Synop.* **1997**, 168.

(3) Tsuge, A.; Araki, T.; Noguchi, Y.; Yasutake, M.; Moriguchi, T.; Sakata, K. *Chem. Lett.* **1998**, 603.

(4) Tsuge, A.; Yamasaki, T.; Moriguchi, T.; Matsuda, T.; Nagano, Y.; Nago, H.; Mataka, S.; Kajigaeshi, S.; Tashiro, M. *Synthesis* **1993**, 205.

(5) Haenel, M.; Staab, H. A. *Chem. Ber.* **1973**, 106, 2203.

(6) Golden, J. H. *J. Chem. Soc.* **1961**, 3741.

(7) Yamato, T.; Miyazawa, A.; Tashiro, M. *Chem. Ber.* **1993**, 126, 2505.

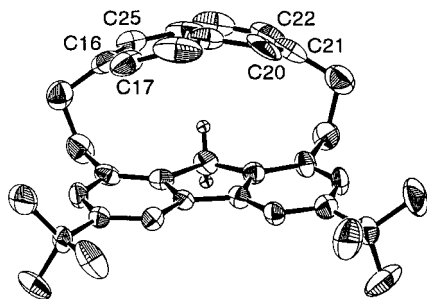


Figure 1. Perspective view of **5b**.

Table 2. Absorption and Fluorescence Spectra^a

| compd | absorption $\lambda_{\text{max}}/\text{nm}$ | fluorescence ^b $\lambda_{\text{max}}/\text{nm}$ (intensity) ^c |
|----------------|--|--|
| 5a | 243, 310 | 342 (23), 354 (26) |
| 5b | 247, 311 | 355 (171) |
| 1b + 2b | 270, 303 | 330 (4), 345 (5) |
| 6a | 389, 412 | 428 (364), 446 (423) |
| 6b | 383, 404 | 418 (1580), 438 (1845) |
| 1b + 3b | 379, 401 | 413 (13), 433 (17) |
| 7a | 341, 357 | 390 (128), 410 (120) |
| 7b | 328, 344 | 400 (178), 415 (160) |
| 1b + 4b | 283, 344 | 382 (72), 395 (50) |

^a 2.0×10^{-4} mol dm⁻³ in CHCl₃. ^b 310 nm excitation. ^c Relative intensity.

orientation as in the fluorenophanes shown here; thus, their spectral behavior has been examined as shown in Table 2.

All the fluorenophanes exhibit a bathochromic shift as compared to the corresponding reference compounds, which can probably be ascribed to a transannular interaction⁹ between the fluorene and the polynuclear aromatic components. Such a shift due to the extent of conjugation has been well-known in the cyclophane system.

Although the fluorene unit and the polynuclear aromatic component in the fluorenophanes (**5b–7b**) seem to be located in closer proximity than those in the dithiafluorenophanes (**5a–7a**), the dithiafluorenophanes show a greater bathochromic shift than the corresponding fluorenophanes. One of the reasons for the hypsochromatic shift in contrast to expectation is the bent aromatic component such as the naphthalene component as shown in Figure 1. The dihedral angle between the plane (C16–C25–C17) and the plane (C21–C20–C22) is 135.2°.

The fluorene **1b** itself shows weak fluorescence. However, as shown in Figure 2, **6b** upon excitation at 310 nm exhibits a strong emission at 438 nm, which corresponds to the band of the anthracene component. A similar fluorescence enhancement can also be observed for **6a**; however, the intensity of the emission is almost one-fourth of that in **6b**. A similar trend in the fluorescence spectrum was confirmed for the fluorenophanes having naphthalene (**5a, 5b**) and pyrene components (**7a, 7b**) (Table 2).

In these systems, the dithiafluorenophanes exhibit weaker emission than the corresponding fluorenophanes, which can be ascribed to flexibility of the molecule and bending of the aromatic unit, since bending of aromatics is well-known to enhance the rate of internal conversion. These results are probably ascribed to a very efficient

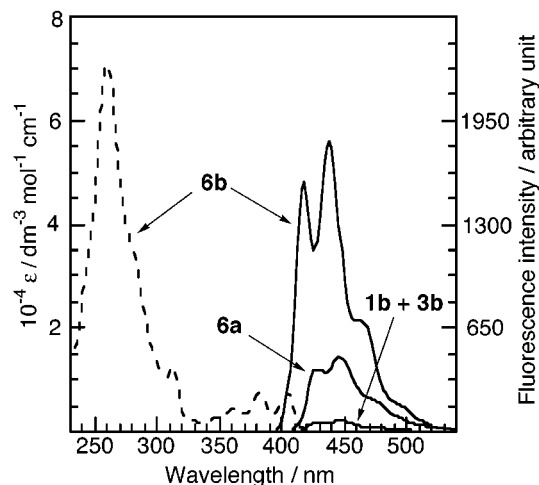


Figure 2. Absorption (dashed line) of fluorenophane **6b** and emission (full line) of fluorenophanes **6a, 6b** and the mixture of **1b** and **3b**.

intramolecular energy transfer¹⁰ from the fluorene component to the anthracene component, since the emission upon the excitation at 310 nm for the 1:1 mixture of **1b** and the reference polynuclear aromatic compounds is negligible as also shown in Figure 2.

A detailed investigation of this intramolecular energy transfer in terms of dynamic structure and the orientation of the two aromatic units of the fluorenophanes is now under progress in our laboratory.

Conclusion

The results obtained in this study reveal that the conformational properties of the 1,8-bridged fluorenophanes consisting of naphthalene, anthracene, and pyrene components depend on their molecular structure, especially the structure of the polynuclear aromatic component, and one of the 9-H protons undergoes a strong shielding effect by the opposite aromatic component. We have shown that the bathochromic shift of the fluorenophanes originated from the transannular interaction between two aromatic components. The fluorenophane compounds in which the fluorene and polynuclear aromatic components are fixed in an appropriate position exhibit characteristic fluorescence behavior that might be based on an efficient energy transfer from the fluorene component to the aromatic component.

Experimental Section

General Methods. All melting points are uncorrected. ¹H NMR spectra were recorded at 500 MHz in CDCl₃ with Me₄Si as internal reference. *J* values are given in Hz. Mass spectra were obtained at 75 eV using a direct-inlet system. Column chromatography was carried out on silica gel (Wako gel, C-300).

Typical Procedure for Coupling Reaction. A solution of **1a** (7.4 g, 20 mmol) and **2a** (6.28 g, 20 mmol) in a mixture of ethanol and benzene (500 mL) was added dropwise from a Hershberg funnel with stirring to a refluxing mixture of CsOH (purity; 80%) (9.84 g, 50 mmol) and NaBH₄ (1.5 g, 40 mmol) in ethanol (3 L). When the addition was complete (24 h), the reaction mixture was concentrated and the residue was extracted with CH₂Cl₂. The extract was dried over MgSO₄, concentrated and chromatographed using 2:1 mixture of chloroform and

(9) Yamato, T.; Fujita, K.; Shinoda, N.; Noda, K.; Nagano, Y.; Arimura, T.; Tashiro, M. *Res. Chem. Intermed.* **1996**, *22*, 871.

(10) Ballardini, R.; Balzani, V.; Dehaen, W.; Dell'Erba, A. E.; Raymo, F. M.; Stoddart, J. F.; Venturi, M. *Eur. J. Org. Chem.* **2000**, 591.

hexane as an eluent to give **5a** (5.95 g, 57%) as colorless prisms (1:1 mixture of chloroform/hexane): mp 195–196 °C; $^1\text{H NMR}$ δ 1.45 (18H, s), 1.58 (2H, s), 3.22 (4H, s), 3.65 (4H, s), 7.04 (2H, dd, $J = 1.5, 8.0$), 7.16 (2H, d, $J = 1.5$), 7.30 (2H, d, $J = 8.0$), 7.49 (2H, d, $J = 1.8$), 7.57 (2H, d, $J = 1.8$); MS m/z 522 (M^+). Anal. Calcd for $\text{C}_{35}\text{H}_{38}\text{S}_2$: C, 80.40; H, 7.34. Found: C, 80.16; H, 7.33.

6a: yield 43%; pale yellow powder (a mixture of chloroform and hexane); mp 184–187 °C; $^1\text{H NMR}$ δ 1.27 (18H, s), 1.37 (2H, s), 3.69 (4H, s), 4.95 (4H, s), 6.99 (2H, d, $J = 1.8$), 7.41 (2H, d, $J = 1.8$), 7.50 (4H, dd, $J = 3.0, 6.8$), 8.36 (4H, dd, $J = 3.0, 6.8$); MS m/z 572 (M^+). Anal. Calcd for $\text{C}_{39}\text{H}_{40}\text{S}_2$: C, 81.76; H, 7.05. Found: C, 81.55; H, 7.09.

7a: yield 35%; white powder (a mixture of chloroform and hexane); mp 199–201 °C; $^1\text{H NMR}$ δ 1.03 (2H, s), 1.40 (18H, s), 1.49 (18H, s), 2.94 (2H, d, $J = 14$), 2.98 (2H, d, $J = 14$), 4.24 (2H, d, $J = 13$), 4.71 (2H, d, $J = 13$), 7.22 (2H, d, $J = 1.8$), 7.42 (2H, d, $J = 1.8$), 7.75 (2H, s), 7.87 (2H, d, $J = 1.5$), 8.17 (2H, d, $J = 1.5$); MS m/z 708 (M^+). Anal. Calcd for $\text{C}_{49}\text{H}_{56}\text{S}_2$: C, 82.98; H, 7.98. Found: C, 82.84; H, 7.99.

Typical Procedure for Pyrolysis. After oxidation of **5a** with *m*-chloroperoxybenzoic acid in CH_2Cl_2 , the resultant tetraoxide (1.60 g, 2.7 mmol) was pyrolyzed at 450 °C under reduced pressure (0.6 Torr) according to the reported method. The crude product was dissolved in CH_2Cl_2 and chromatographed with a 1:5 mixture of chloroform and hexane as an eluent, giving crude **5b**. Recrystallization from a mixture of chloroform and hexane afforded **5b** (0.50 g, 40%) as colorless prisms: mp 216–218 °C; $^1\text{H NMR}$ δ -0.69 (1H, d, $J = 21$), 1.43 (18H, s), 1.61–1.97 (2H, m), 2.11 (1H, d, $J = 21$), 2.61–3.28 (6H, m), 5.95 (1H, dd, $J = 1.5, 8.0$), 6.51 (1H, s), 6.70 (1H, d, $J = 8.0$), 7.07 (1H, d, $J = 1.5$), 7.12 (1H, d, $J = 1.5$), 7.28 (1H, dd, $J = 1.5, 8.0$), 7.54 (1H, d, $J = 1.8$), 7.58 (1H, d, $J = 1.8$), 7.76 (1H, s), 7.83 (1H, d, $J = 8.0$);

MS m/z 458 (M^+). Anal. Calcd for $\text{C}_{35}\text{H}_{38}$: C, 91.63; H, 8.37. Found: C, 91.46; H, 8.38.

6b: yield 25%; pale yellow needles (ethanol); mp 210–215 °C; $^1\text{H NMR}$ δ -1.59 (1H, d, $J = 21$), 1.43 (18H, s), 1.83 (1H, d, $J = 21$), 2.27–2.33 (2H, m), 3.15–3.20 (2H, m), 3.49–3.55 (2H, m), 4.26–4.31 (2H, m), 6.38 (2H, dd, $J = 3.2, 6.8$), 6.93 (2H, dd, $J = 3.2, 6.8$), 7.13 (2H, d, $J = 1.8$), 7.23 (2H, d, $J = 1.8$), 7.61 (2H, dd, $J = 3.2, 6.8$), 8.53 (2H, dd, $J = 3.2, 6.8$); MS m/z 508 (M^+). Anal. Calcd for $\text{C}_{39}\text{H}_{40}$: C, 92.06; H, 7.94. Found: C, 91.92; H, 7.98.

7b: yield 40%; colorless prisms (ethanol); mp 230–234 °C; $^1\text{H NMR}$ δ -0.80 (1H, d, $J = 21$), 1.13 (9H, s), 1.38 (9H, s), 1.44 (9H, s), 1.61 (1H, d, $J = 21$), 1.64 (9H, s), 2.84–4.10 (8H, m), 6.39 (1H, s), 7.04 (1H, d, $J = 1.8$), 7.06 (1H, d, $J = 1.8$), 7.12 (1H, d, $J = 1.8$), 7.24 (1H, d, $J = 1.8$), 7.28 (1H, d, $J = 1.5$), 7.36 (1H, d, $J = 1.5$), 7.89 (1H, s), 8.09 (1H, d, $J = 1.5$), 8.32 (1H, d, $J = 1.5$); MS m/z 644 (M^+). Anal. Calcd for $\text{C}_{49}\text{H}_{56}$: C, 91.23; H, 8.77. Found: C, 91.09; H, 8.82.

X-ray Analysis. Crystal data for **5b**: $\text{C}_{35}\text{H}_{38}$, M 458.69, monoclinic, space group $P2_1/a$ (No. 14), $a = 19.84(1)$ Å, $b = 6.041(5)$ Å, $c = 23.58(1)$ Å, $\alpha = 90^\circ$, $\beta = 107.58(5)^\circ$, $\gamma = 90^\circ$, $V = 2693(3)$ Å³, $Z = 4$, $\rho = 1.13$ g/cm³. A total of 6985 unique data points ($\theta_{\text{max}} = 27.5^\circ$) were measured at $T = 296.2$ K on a Rigaku AFC7R diffractometer (Mo $K\alpha$ radiation; $\lambda = 0.7107$ Å). Numerical absorption correction was applied ($\mu = 0.63$ mm⁻¹). The structure was solved by direct methods and refined by the full-matrix least-squares methods on F with anisotropic temperature factors for non-hydrogen atoms using the TeXsan package. The final R and R_w values are 0.0758 and 0.0429 for 1428 reflections with $I > 3.0\sigma(I)$ and 354 parameters.

JO010632J